Nuclear Engineering and Technology 54 (2022) 1909–1913

Contents lists available at ScienceDirect

Nuclear Engineering and Technology

journal homepage: www.elsevier.com/locate/net

Technical Note

Uranium tetrafluoride production at pilot scale using a mercury electrode cell

Munir Dides, José Hernández*, Luis Olivares

Chilean Nuclear Energy Commission (CChEN), Santiago, Chile

ARTICLE INFO

Article history:
Received 10 September 2021
Received in revised form
5 November 2021
Accepted 14 November 2021
Available online 17 November 2021

Keywords:
Uranium tetrafluoride
Electrolysis
Mercury electrode

ABSTRACT

This work shows the technical feasibility to obtain uranium tetrafluoride through an electrochemical mercury cell. This technique represents a custom scaling-up methodology from our previous studies to obtain UF_4 using the dropping mercury electrode cell. The UF_4 products were obtained from natural UF_6 gas, which was hydrolyzed to obtain a 50 g/L UO_2F_2 solution. The electrolysis cell was made using a mercury reservoir, to reach UF_4 production rates of 1 Kg UF_4/day. This custom design allowed a stable UF_4 production thanks to the mercury cathode, which do not permit the accumulation of solid products in its surface. The cell was tested using current densities from 5.000 to 17.500 A/m^2 and temperatures from 25 to 65 °C. The maximum current efficiency achieved under these conditions was 80%. The UF_4 powders possessed spherical morphology, with diameters between 20 and 80 μm. Compared to the $SnCl_2$ precipitation, this process did not allow preferential growth of the precipitates. This improved the compaction of the UF_4 – Mg powders mixtures, with densities between 3.0 and 3.5 g/cm^3. The purity of the UF_4 products was over 98%.

1. Introduction

1.1. Radiopharmaceuticals

The Chilean Nuclear Energy Commission, CCHEN, produces in its Materials Testing Reactor (MTR) RECH-1, radioisotopes of use in nuclear medicine, such as ^{99m}Tc and ^{131}I. The radioisotope for medical use technetium–99 metastable (^{99m}Tc), a product of the radioactive decay chain of ^{99}Mo, is the radioisotope with the highest use in nuclear medicine in the world. This radioisotope is used in medical diagnostic procedures of various pathologies, concentrating around 80% of all the images obtained by gamma cameras of the nuclear medicine, corresponding to more than 25 million studies per year. In Chile, it is applied in more than 90% of nuclear medicine studies (about 200,000 patients). In Santiago, ^{99m}Tc is produced by neutron activation of molybdenum. Outside from Santiago, ^{99m}Tc is imported from external generators [1,2]. To use uranium for radiopharmaceuticals manufacturing, uranium concentrates must be converted to suitable compounds by further purification and forming processes steps in the fuel cycle. Fig. 1 presents the conventional refining and conversion route to obtain UF_6 using aqueous processes, usually known as the “wet route” [3,4].

Uranium metal is required to produce uranium fuels based on intermetallic compounds, such as UAl_3, U_3Si_2; which are then used to fabricate LEU (Low Enriched Uranium) fuels. Uranium metal is also required to produce LEU fuels-based irradiation targets for ^{99}Mo radioisotope production, for radiopharmaceutical manufacturing. LEU poses restrictions on its quantity due to criticality considerations, and hence its preparation (commonly by metallothermic reduction of UF_4) needs to be carried out at small scale [5]. This work proposes an alternative method to increase the production of UF_4 powders, based on a mercury cell.

Mercury can be used as catalyzer to obtain metallic species of low reduction potential in aqueous solutions [6–9]. Unfortunately, the electrodes based on this metal are not scalable to use for electrochemical reactions for mass production, commonly because of environmental issues [10]. Therefore, the development of electrochemical cells, keeping the features of Hg, is required for practical applications [11]. Uranium tetrafluoride has been normally obtained in our facilities by chemical precipitation, introducing in a stirred reactor 20 lt. of an uranyl fluoride (UO_2F_2) solution, containing 1.250 g U, plus dissolved $SnCl_2$ as reducing agent and hydrofluoric acid, HF, according to reaction (1) [12]:

* Corresponding author. Chilean Nuclear Energy Commission (CChEN). Av. Bilbao, 12501, Chile.
E-mail address: jose.hernandez@cchen.cl (J. Hernández).

https://doi.org/10.1016/j.net.2021.11.013

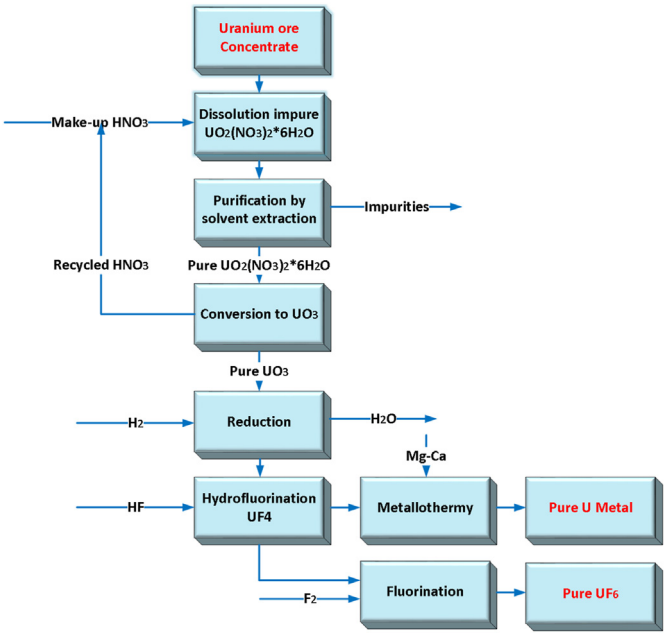

Fig. 1. Stages in conventional (wet route) UF_6 refining-conversion process.

$$UO_2F_2 + SnCl_2{*}2H_2O + 4HF \rightarrow UF_4{*}H_2O + SnCl_2F_2 + 3H_2O \quad (1)$$

The electrochemical reduction process have several advantages over the chemical precipitation reactions: the production rate and the grain size of the products can be controlled through temperature and the current density. Besides, this process does not use additional reagents for the chemical reaction. For these reasons, this method can improve the performance of all the subsequent uranium purification stages, either to obtain uranium-based fuel plates for research reactors or uranium pellets for power reactors [13]. This study will describe this alternative procedure to obtain UF_4 using a mercury cathode-based process.

2. Experimental development

Fig. 3 shows the experimental process to obtain natural UO_2F_2 solutions using a hydrolyzer equipment. At room temperature, UF_6 is solid and requires raising the temperature above 56 °C to

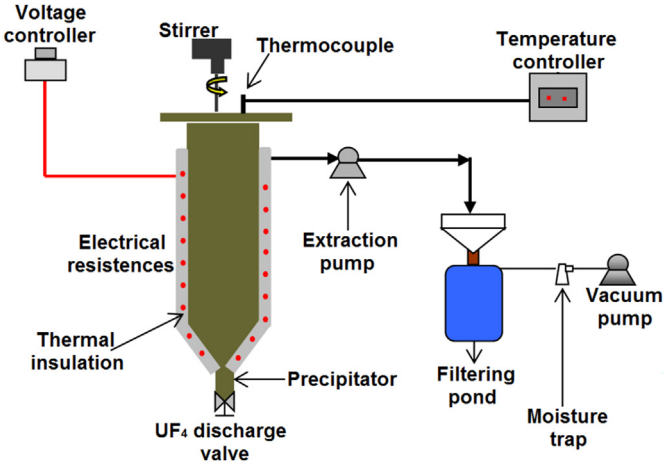

Fig. 2. UF_4 precipitation reactor.

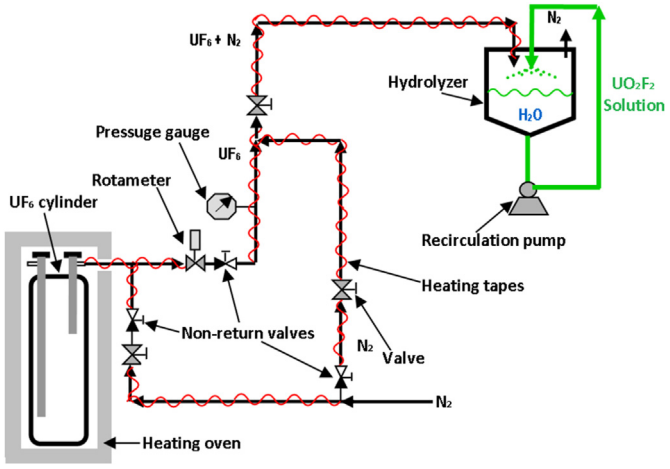

Fig. 3. Hydrolyzer system for UO_2F_2 production.

sublimate it. The increase in pressure in the container drives it out and conduct it through Monel 400 ducts, using N_2 as gas drag, until entering the hydrolyzer, where it is contacted with H_2O in the form of a fine drizzle reacting with fast kinetic, according to equation (2):

$$UF_6 + H_2O = UO_2F_2 + HF \quad (2)$$

Due to the toxicity risks of UF_6 and the HF formation in contact with environmental humidity, it is necessary the confinement of the equipment and in depression, so a cabin with constant extraction was designed and built in order to ensure a depression of 5–10 mm of water column with an external gas scrubber system. This process generated UO_2F_2 solutions with a concentration of 50 g/l of uranium and pH 1.0–1.5 were prepared.

The Hg was placed at the bottom of the cell and the electrical connection to the negative terminal was made of iron covered with acrylic to protect it from the UO_2F_2 corrosion. A bridge was installed with two Pt electrodes connected to the positive terminal. The solution was heated to temperatures between 25 and 65 °C. The temperature of the system must not exceed 65 °C, because of the increase in HF evaporation rate. Under these conditions, the HF evaporation rate was estimated using the method described by Kawamura and Mackay [14], giving a rate of 0.0882 g/min. However, to decrease this effect, the surface of the solution was covered with polystyrene balls. These balls reduced the effective evaporation area to 21.5% of the original value, giving an effective evaporation rate of 0.0189 g/min.

To prevent mercury evaporation, the cell was sealed inside a Lexan box and a sulphide carbon trap for mercury adsorption. This prevented any possible mercury leaking from the cell. Although the vapor pressure of mercury is low (0.002 mm Hg) at 24 °C, an atmosphere fully saturated with mercury vapor contains approximately 18 mg/m^3, which can be dangerous to health. Table 1 shows the chemical analysis of the UO_2F_2 solution. These impurities come from the previous chemical purification processes. It is important to trace them, because they also undergo neutron activation, which decreases the radiopharmaceutical production efficiency. The chemical analyses were done using the ICP-mass spectrometry.

All the experiments were carried out using a KXN-15100D DC

Table 1
Chemical analysis of the main impurities of the UO_2F_2 solution.

Impurities	Al	B	Cd	C	Cu	Fe	Mn	Si
ppm	15	18	21	5	15	23	24	11

power supply, in galvanostatic mode. The custom mercury cell of Fig. 4 can operate continuously and with low mercury volumes. This made the cell easy to control, scalable and safer than the methods used in analytical chemistry, and the conventional mercury cell. The mercury compartment at the bottom decreases the need of high volumes for this element. The mercury - UO_2F_2 solution served as the cathode of the cell. The cathodic reaction was according to reaction (3):

$$UO_2^{2+} + 4H^+ + 4F^- + 2e^- \rightarrow UF_4 + 2H_2O \quad (3)$$

The current efficiency of each experiment was calculated according to equation (4):

$$Current\ efficiency = \frac{Faraday's\ law}{Mass\ of\ UF_4\ product} = \frac{\frac{I*t*MW_{UF_4}}{n*F}}{Mass\ of\ UF_4} \quad (4)$$

where I is the current intensity, t is time, MW_{UF_4} is the molar weight of UF4, n is the change of oxidation number, and F is the faraday number. The anodic connection for water oxidation was made through Pt wires, and hermetically insulated to avoid corrosion on the upper section of the wire, equation (5):

$$H_2O \rightarrow \frac{1}{2}O_2 + 2H^+ + 2e^- \quad (5)$$

Hydrogen evolution took place as a secondary reaction in the mercury cathode, equation (6):

$$H^+ + e^- \rightarrow \frac{1}{2}H_2 \quad (6)$$

This configuration allowed obtaining 5 Kg of UF_4 continuously per week. After every day, the mercury was drained using vacuum pumps and filtered to recover the UF_4 obtained. The UO_2F_2 solution was restored to its original composition by adding UO_3 and HF for every test. The UF_4 powders obtained were separated from the mercury using a peristaltic pump and filtrating, and it was washed using deionized water. Subsequently, it was dried at 70–80 °C in an air-nitrogen atmosphere, then it was dehydrated in an inert atmosphere, obtaining a product with a water content of less than 0.1%. The dehydrated product was weighed and stored in polycarbonate jars. The products obtained was characterized through XRD and chemical analysis of impurities using ICP-Mass Spectrometry. The grain size of the UF_4 powder samples obtained was measured by laser diffraction using a Particle Size Analyzer for powder materials Mastersizer 3000E Hydro EV, with a measurement range of 0.1–1000 μm.

An important aspect of any mercury cell system is its stability in time. Theoretically, there is no mercury consumption during the electrolysis process. However, the mercury electrode tends to oxidize to HgO, according to equation (7) [15]:

$$Hg_{(l)} + \frac{1}{2}O_2 \rightarrow HgO_{(s)} \quad (7)$$

For this reason, any kind of mercury cell needs careful control of Hg flow and possible Hg oxidation. This reaction can take place any time when the mercury losses contact with the cathodic connection, because of the mercury flow in the process. However, since the mercury was stagnant in the proposed system and the mercury itself was confined into a small compartment (Fig. 4), the mercury loss by this mechanism were minimal.

3. Results and discussions

Fig. 5 shows the influence of the cathodic current density and temperature over the current efficiency of the process. Both parameters have important consequences over the current efficiency. Although the temperature improves the current efficiency in all cases because of the reduction in the ohmic resistance of the HF solution, it is not safe to increase it over 65 °C. The system can work at higher temperatures, but it is not recommendable due to the effect of HF evaporation. The reason for the loss of current efficiency was the protons reduction to hydrogen, reaction (6). This was verified in the final pH value of the UO_2^{2+} solution, which ranged from 2.5 to 4.0. Since this parameter can lead to uranium precipitation, HF acid and UO_2F_2 were replenished after every 24 h test.

Fig. 6 illustrates the effect of the cathodic current density and temperature over the grain size of the UF_4 samples. Although high current densities and temperatures decrease the cell efficiency, these conditions also decrease the grain size of the UF_4 samples. Low grain sizes of UF_4 powders allows reaching UF_4 – Mg (or Ca) mixtures with densities between 3.0 and 3.5 g/cm^3. This benefits the subsequent metallothermy process to obtain uranium ingots free of porosities.

According to the electro-crystallization theory, the formation of precipitates can also be studied using the classical nucleation and grow mechanisms. Equation (8) shows the Gibbs free energy for

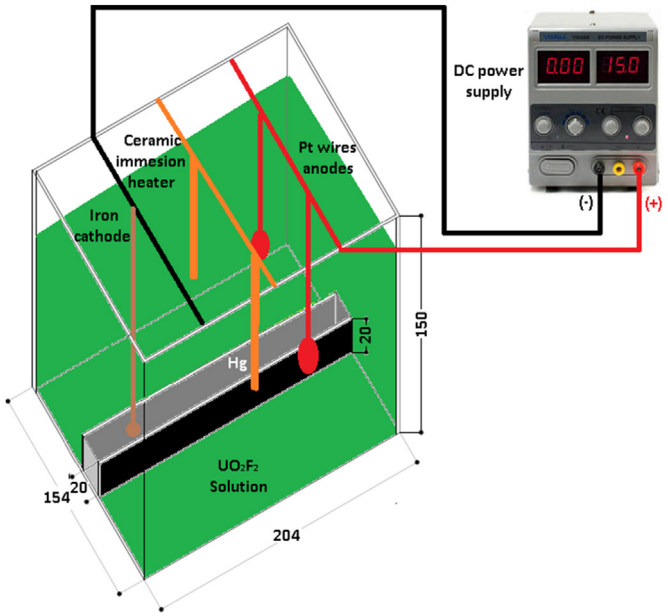

Fig. 4. Custom mercury cell used, measures in mm.

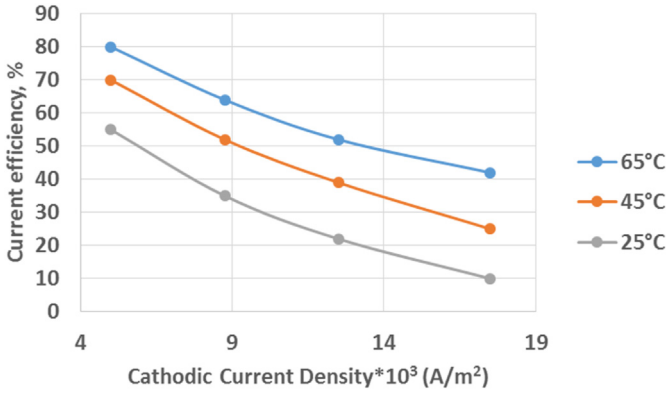

Fig. 5. Current efficiency v/s cathodic current density.

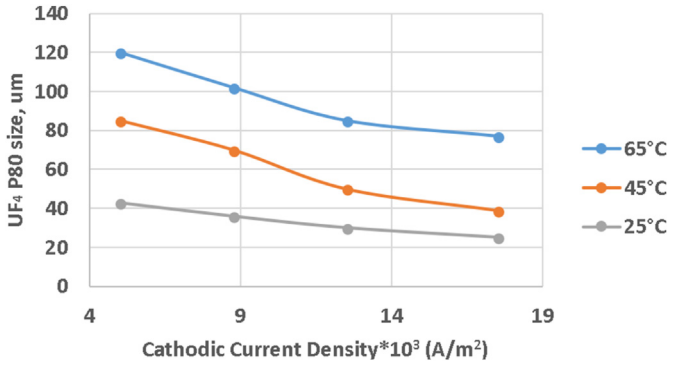

Fig. 6. UF_4 powders P80 size v/s cathodic current density.

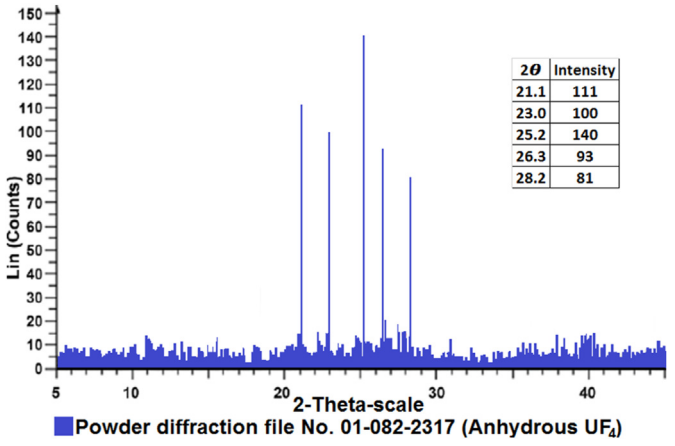

Fig. 7. X-ray diffraction profile of UF_4 sample, showing the characteristic UF_4 peaks, identified according to 01-082-2317 anhydrous pattern (X'Pert Highscore software).

nucleation [16,17]:

$$\Delta G_{nucl} = -\frac{4}{3}\pi r^3(-\Delta G_V) + 4\pi r^2\theta \tag{8}$$

where ΔG_{nucl} is the free energy for nucleation, r is the size of the initial nucleus, ΔG_V is the is the Gibbs free energy change when a soluble specie is adsorbed to the surface, compared to being in the supersaturated electrolyte, and θ is the interfacial area. However, in the case of an electrochemical system, ΔG_V is related to the electrochemical system, equation (9):

$$\Delta G_V = -nF|\eta| \tag{9}$$

where η is the cathodic overpotential of the cell. Therefore, the critical radius r_{crit} will be:

$$r_{crit} = \frac{2\theta}{nF|\eta|} \tag{10}$$

Equation (10) shows that, high overpotentials, caused by high currents applied using the DC power source, decrease the critical radius of the UF_4 precipitation, giving as result, fine powders of the precipitate. Accordingly, the temperature influences the overpotential, given by equation (11):

$$\eta = E - E_0 = \frac{kT}{ze}\ln\left(\frac{a_{ads}}{a^0_{ads}}\right) \tag{11}$$

Table 2
Chemical analysis of the main impurities in UF_4 powders.

Impurities	Al	B	Cd	C	Cu	Fe	Mn	Si	UF_4
ppm	10	12	15	0.5	13	19	18	5	>98%

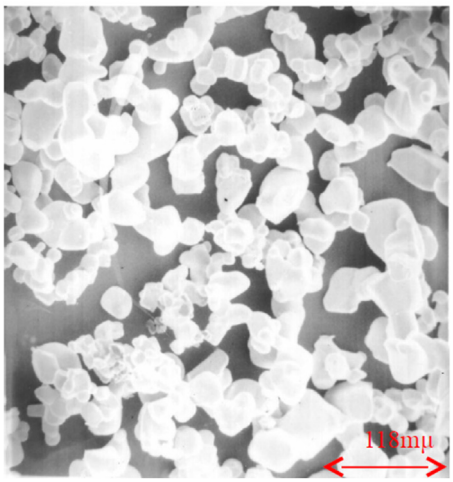

Fig. 8. SEM image of a UF_4 sample.

where a^0_{ads} is the activity of the ad-layer formed on the foreign substrate at the equilibrium potential, E_0. In other words, temperature contributes directly to decrease the overpotential required to reach a determined current density. For this reason, temperature has the opposite effect of the current intensity, increasing the grain size of the UF_4 samples, and therefore, decreasing its bulk density.

Fig. 7 shows the XRD of a UF_4 sample. The X-ray diffraction analysis shows anhydrous UF_4 as the main product. Table 2 shows the chemical composition of the UF_4 sample.

Figs.8 and 9 show different UF_4 samples, obtained both from the proposed mercury cell electrode and the conventional $SnCl_2$ precipitation. It was found that the shape of the particles obtained using the mercury cell were essentially spherical. Fig. 9 shows a UF_4 sample obtained by conventional chemical reduction, using the $SnCl_2$ chemical process from Fig. 2. This UF_4 particles possessed a

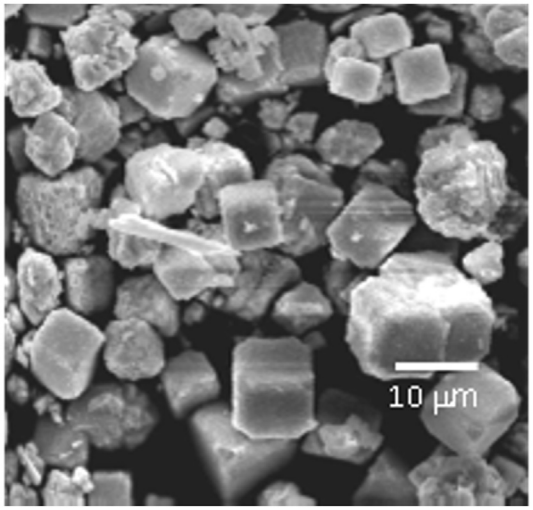

Fig. 9. UF_4 sample obtained, using $SnCl_2$ as reducing agent.

cubic shape morphology, which denotes a homogeneous growth [18–20], because of the creation of new surfaces during the precipitation reaction during the nucleation and growth mechanisms. The spherical shape of the UF_4 samples obtained by the proposed mercury cell allowed producing an additional mass of 10–15% in the magnesiothermy reactor, by decreasing the presence of porosities inside the powders.

4. Conclusions

The main conclusions for this work were the followings:

- The proposed mercury cell allowed obtaining UF_4 powders from UO_2F_2 solutions by controlling the cathodic current density and the temperature of the system.
- Although mercury can be toxic for human health, the design of the proposed mercury cell allows the production of UF_4 powders using a minimum volume of mercury in the reservoir at the bottom of the cell.
- The proposed mercury cell allowed working continuously during 24 h, with an acid make-up after every test and avoiding the mercury oxidation to HgO.
- The up-to-date UF_4 precipitation using $SnCl_2$ requires a size reduction stage to achieve the desired grain size for the UF_4 powders. This mercury cell process obtained UF_4 in a single stage to the later metallothermic reduction for the manufacture of uranium fuels, by controlling the temperature and current density.

Declaration of competing interest

The authors declare that they have no known competing financial interests or personal relationships that could have appeared to influence the work reported in this paper.

Acknowledgments

The authors would like to thank the Chilean Nuclear Energy Commission (ID: CChEN, for its Spanish abbreviation) for their economic support, during every stage of the project.

References

[1] J. Lisboa, M. Barrera, J. Marin, Fabricacion de blancos anulares para Mo-99 utilizando láminas de uranio natural, uranio LEU, Niquel y aluminio estructural Al-3003, in: Iberomet XI, X CONAMET/SAM, Viña del mar, Chile, 2010.
[2] J. Lisboa, J. Marin, M. Barrera, I. Escobar, D. Mena, Recubrimiento de laminas de uranio mediante electrodeposicion de Ni para uso en la produccion de Mo de fision, in: 11° Congreso Binacional de Metalurgia y Materiales, SAM/CONAMET, Rosario, Argentina, 2011.
[3] International Atomic Energy Agency, Nuclear Fuel Cycle Information System, 2009. Vienna, Austria.
[4] K. Huff, Introduction to nuclear power economics, in: Economics of Advanced Reactors and Fuel Cycles, Elsevier Inc., Urbana, IL, United States, 2019, pp. 1–20.
[5] S. Gupta, R. Kumar, S. Satpati, M. Sahu, Effect of oxygen containing compounds in uranium tetrafluoride on its non-adiabatic calciothermic reduction characteristics, Nucl. Eng. Technol. 53 (2021) 1931–1938.
[6] S. Danielle, Anodic stripping, in: VOLTAMMETRY/Anodic Stripping, Elsevier, Ltd, 2005, pp. 5422–5425.
[7] W. Hansen, Preparation of binary compounds of uranium and thorium, 13 Sept 1966. USA Patent US3272601.
[8] N. Brandon, P. Francis, J. Jeffrey, G. Kelsall, Q. Yin, Thermodynamics and electrochemical behavior of Hg-S-Cl-H2O systems, J. Electroanal. Chem. 497 (2001) 18–32.
[9] Y. Lee, C. Hu, Mercury drop electrodes, in: Encyclopedia of Applied Electrochemistry, Springer Science Business, New York, 2014, pp. 1233–1239.
[10] Y. Mikkelsen, K. Schroder, Amalgam electrodes for electroanalysis, Electroanalysis 15 (8) (2003) 679–687.
[11] S. Abbas, S. Kim, H. Saleem, S. Ahn, K. Jung, Preparation of metal amalgam electrodes and their selective electrocatalytic CO2 reduction for formate production, Catalysts 9 (367) (2019) 1–13.
[12] P. Rojas, H. Contreras, A. Garrao, F. Valdés, Obtaining metallic uranium from UF6, in: International Meeting on Reduced Enrichment of Research and Test Reactors - RERTR, Santiago, Chile, 2011.
[13] "Fuel Fabrication," United States Nuclear Regulatory Commission [Online]. Available: https://www.nrc.gov/materials/fuel-cycle-fac/fuel-fab.html. (Accessed 20 December 2020).
[14] P. Kawamura, D. Mackay, The evaporation of volatile liquids, J. Hazard Mater. 15 (1987) 343–364.
[15] W. Zhen, L. Jing, Y. Yingju, L. Feng, D. Junyan, Heterogeneous reaction mechanism of elemental mercury oxidation by oxygen species over MnO2 catalyst, Proc. Combust. Inst. 37 (3) (2019) 2967–2975.
[16] Y. Liu, X. Xu, M. Sadd, O. Kapitanova, V. Krivchenko, J. Ban, J. Wang, X. Jiao, Z. Song, J. Song, S. Xiong, A. Matic, Insight into the critical role of exchange current density on electrodeposition behavior of lithium metal, Adv. Sci. 8 (5) (2021) 1–11.
[17] A. Milchev, Electrochemical phase formation on a foreign substrate-basic theoretical concepts and some experimental results, Contemp. Phys. 32 (5) (1991) 321–332.
[18] S. Rej, M. Bisetto, A. Naldoni, P. Fornasiero, Well-defined Cu2O photocatalysts for solar fuels and chemicals, J. Mater. Chem. 9 (2021) 5915–5951.
[19] A. Barnard, Modeling polydispersive ensembles of diamond nanoparticles, Nanotechnology 24 (2013) 1–14.
[20] P. Geysermans, F. Finocchi, J. Goniakowski, R. Hacquart, J. Jupille, Combination of (100), (110) and (111) facets in MgO crystals shapes from dry to wet environment, Phys. Chem. Chem. Phys. 11 (2009) 2228–2233.